Proceedings of the 6th International Conference on Gas Hydrates (ICGH 2008), Vancouver, British Columbia, CANADA, July 6-10, 2008.

COMPUTATIONAL CHARACTERIZATION OF 13C NMR LINESHAPES OF CARBON DIOXIDE IN STRUCTURE I CLATHRATE HYDRATES

Saman Alavi,* Peter Dornan, and Tom K. Woo
Department of Chemistry, University of Ottawa, Ottawa, ON, K1N 6N5, CANADA

ABSTRACT

Nonspherical large cages in structure I (sI) clathrates impose non-uniform motion of nonspherical guest molecules and anisotropic lineshapes in NMR spectra of the guest. In this work, we calculate the lineshape anisotropy of the linear CO_2 molecule in large sI clathrate cages based on molecular dynamics simulations of this inclusion compound. The methodology is general and does not depend on the temperature and type of inclusion compound or guest species studied. The nonspherical shape of the sI clathrate hydrate large cages leads to preferential alignment of linear CO_2 molecules in directions parallel to the two hexagonal faces of the cages. The angular distribution of the CO_2 guests in terms of a polar angle θ and azimuth angle ϕ and small amplitude vibrational motions in the large cage are characterized by molecular dynamics simulations at different temperatures in the stability range of the CO_2 sI clathrate. These distributions are used to calculate the NMR powder spectrum of CO_2 at different temperatures. The experimental ^{13}C NMR lineshapes of CO_2 guests in the large cages show a reversal of the skew between the low temperature (77 K) and the high temperature (238 K) limits of the stability of the clathrate. Good agreement between experimental lineshapes and calculated lineshapes is obtained. No assumptions regarding the nature of the guest motions in the cages are required.

Keywords: gas hydrates, chemical shift anisotropy, carbon dioxide clathrate

NOMENCLATURE

γ magnetogyric ratio
$\boldsymbol{\sigma}$ chemical shielding tensor
$\mathbf{B}_0$ external magnetic field strength
$\boldsymbol{\sigma}_{\mathbf{PA}}$ chemical shielding tensor in principle axis frame
$\boldsymbol{\sigma}_{\mathbf{LAB}}$ chemical shielding tensor in laboratory frame
σ_{ii} eigenvalues of chemical shielding tensor in PA frame (i = 1,2,3)
$\sigma_{\alpha\alpha}$ eigenvalues of chemical shielding tensor in LAB frame ($\alpha = x,y,z$)
$\mathbf{R}(\alpha,\beta,\gamma)$ rotation matrix in terms of Euler angles
$\mathbf{R}(\theta,\phi)$ rotation matrix for linear molecules
$\boldsymbol{\sigma}_{i,\mathrm{LAB}}(T;t)$ lab frame chemical shielding tensor for cage i at time t and temperature T.
$\overline{\sigma}_{i,\alpha\alpha}(T)$ time averaged eigenvalues of $\boldsymbol{\sigma}_{i,\mathrm{LAB}}(T;t)$

INTRODUCTION

NMR chemical shifts and chemical shift anisotropy are widely used to characterize the structure and dynamics of guest species in clathrates.[1-11] A difference between the chemical shift of the guest in the clathrate with the free guest indicates the encapsulation of the guest in the clathrate cages. Peak integration of the NMR spectra of the guests, along with knowledge of the structure and number of cage types in the clathrate allows for the assignment relative populations of the guests in different cages. The chemical shift anisotropy for the guest species at each temperature can be used to characterize the dynamics of guest in the clathrate. The standard method for extracting dynamic information from NMR lineshapes[12] of guest molecules is to assume a model for the guest motion in the cage and fit the adjustable parameters in the model to reproduce the experimental lineshape. Different models for guest dynamics are typically required to match the experimental data at different temperatures.

The dynamics of CO_2 molecules in structure I (sI) clathrates have been characterized using this approach. The sI clathrates have a cubic unit cell composed 46 water molecules arranged in six large 14-sided cages ($5^{12}6^2$) with average cavity radii of 4.33 Å and two 12-sided cages (5^{12}) with average cavity radii of 3.95 Å. The large cages in

* Corresponding author: Phone: +1 613 265 5335 Fax +1 613 998 7833 E-mail: saman.alavi@nrc-cnrc.gc.ca

the sI clathrate are flattened in the direction perpendicular to the two hexagonal faces of the cage and non-spherical guest molecules such as CO_2 will be preferentially aligned with the long axis parallel to the hexagonal faces, as depicted in the inset of Figure 1. This anisotropic spatial distribution leads to incomplete averaging of the chemical shift tensor observed in the ^{13}C NMR spectra of the CO_2 guests in the large cages of the sI clathrate and anisotropic lineshapes shown in Figure 1. In contrast, the more spherically symmetric small cages of the sI clathrate show isotropic NMR lineshapes for the guest molecules.

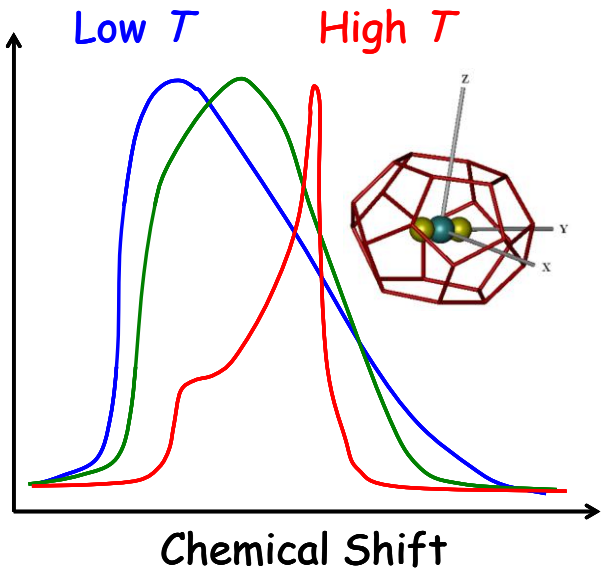

Figure 1. A schematic representation of the anisotropic ^{13}C NMR lineshape for the CO_2 guests in large sI cages at three temperatures. The CO_2 guest in a large cage is shown in the inset.

Figure 1 shows that the ^{13}C NMR lineshapes of CO_2 in the large cages change drastically with temperature. At low temperatures (blue line) the lineshape of CO_2 in the sI large cages has a skew similar to solid α-phase CO_2[12] but with a smaller span. At intermediate temperatures (green line), the skew of the peak is almost zero and at higher temperatures near the decomposition temperature of the clathrate (red line), the direction of the skew of the lineshape is inverted compared to the low temperature line. The span of the peak also decreases at high temperatures. These lineshapes are interpreted in terms of the different spatial distributions and dynamics of CO_2 guests in the large cages at different temperatures.[12,13] Reasonable models describing the angular distribution of the guests in clathrate cages are developed and the adjustable parameters in the model are determined by fitting the predicted lineshapes from these models to experiments. For example, the high temperature motion of CO_2 in the large cages has been modeled[14] by a precessional motion with a maximum range of β_{max} from the equatorial plane, or equivalently with the polar angle θ ranging from $\theta_{min} = 90° - \beta_{max}$ to $\theta_{max} = 90° + \beta_{max}$. Fitting the prediction of this model to the experimentally observed span, a value of $\beta_{max} = 31°$ is obtained for the range of the distribution of the CO_2 guests about the equatorial plane. Different models are obviously required to describe the dynamics of the guest motion at high and low temperature limits.[12]

In this work, we present a molecular dynamics calculation method to determine the spatial orientations of the molecules required for calculating NMR chemical shift anisotropy of guest molecules in clathrates. In this method, no assumptions about the nature of the guest motion is required and a uniform methodology is applicable to all temperatures. Furthermore, the method developed is general and can be used to predict chemical shift anisotropies of guests in other inclusion compounds, pure solid phases with dynamically disordered components, or dynamically mobile side-chains of protein molecules.

The Hamiltonian for a spin-1/2 nucleus in a static external magnetic field $\mathbf{B}_0$ is,

$$H = -\gamma\hbar\mathbf{I}\cdot(\mathbf{1}-\boldsymbol{\sigma})\cdot\mathbf{B}_0 \qquad (1)$$

where $\boldsymbol{\sigma}$ is the second-rank chemical *shielding* tensor, γ is the magnetogyric ratio, $\mathbf{I}$ is the nuclear spin angular momentum operator and $\mathbf{1}$ is the unit tensor.[15]

In the principal axes (PA) coordinate system, the chemical shielding tensor of a molecule is diagonal,

$$\boldsymbol{\sigma}_{PA} = \begin{pmatrix} \sigma_{11} & 0 & 0 \\ 0 & \sigma_{22} & 0 \\ 0 & 0 & \sigma_{33} \end{pmatrix}, \qquad (2)$$

and the principle axis eigenvalues are ordered so that, $\sigma_{11} \le \sigma_{22} \le \sigma_{33}$. The chemical shielding tensor is characterized by the isotropic chemical shielding $\sigma_{iso} = (\sigma_{11} + \sigma_{22} + \sigma_{33})/3$, span $\Omega = \sigma_{33} - \sigma_{11}$, skew $\kappa = 3(\sigma_{iso} - \sigma_{22})/\Omega$, and anisotropy $\Delta = \sigma_{33} - \sigma_{iso}$.[16] Chemical *shifts* are defined as $\delta_{ii} = \sigma_{ref} - \sigma_{ii}$ where σ_{ref} is the isotropic chemical shielding

of a reference material, tetramethylsilane (TMS) in the case of ^{13}C.

In the laboratory frame (LAB), a molecule in a solid is characterized an orientation determined by the three Euler angles α, β, and γ. In the case of weak dipolar coupling between the guest and host cage, the chemical shielding tensor depends only on the molecular orientation and not on the position inside the cage. In the weak coupling limit, the chemical shielding tensor of the guest in the laboratory frame, $\boldsymbol{\sigma}_{\mathrm{LAB}}$, is related to $\boldsymbol{\sigma}_{\mathrm{PA}}$ through the rotation matrix $\mathbf{R}(\alpha,\beta,\gamma)$,

$$\boldsymbol{\sigma}_{LAB}(\alpha,\beta,\gamma) = \mathbf{R}^{-1}(\alpha,\beta,\gamma)\boldsymbol{\sigma}_{PA}\mathbf{R}(\alpha,\beta,\gamma). \quad (3)$$

For linear CO_2, the second-rank chemical shielding tensor in its PA frame in Eq (2) reduces to,

$$\boldsymbol{\sigma}_{PA} = \begin{pmatrix} \sigma_{11} & 0 & 0 \\ 0 & \sigma_{11} & 0 \\ 0 & 0 & \sigma_{33} \end{pmatrix}. \quad (4)$$

The two equal eigenvalues in the directions perpendicular to the molecular axis are shown as σ_{11}. Without loss of generality, the isotropic chemical shielding is chosen as the origin and the chemical shielding tensor is written in traceless form,[17, 18]

$$\boldsymbol{\sigma}_{PA}^{\mathrm{traceless}} = -\sigma_{11}\begin{pmatrix} 1 & 0 & 0 \\ 0 & 1 & 0 \\ 0 & 0 & -2 \end{pmatrix}. \quad (5)$$

In the laboratory frame, with a choice of an external reference *z*-axis, the orientation of a linear molecule is determined by spherical polar angle θ and azimuth angle ϕ and the chemical shielding tensor $\boldsymbol{\sigma}_{\mathrm{LAB}}$, is related to $\boldsymbol{\sigma}_{\mathrm{PA}}$ through the rotation matrix $\mathbf{R}(\theta,\phi)$,

$$\boldsymbol{\sigma}_{LAB}(\theta,\phi) = \mathbf{R}^{-1}(\theta,\phi)\boldsymbol{\sigma}_{PA}\mathbf{R}(\theta,\phi). \quad (6)$$

Using the standard form of the rotation matrices[19] with the principal axis chemical shielding given in Eq (5) we get,

$$\boldsymbol{\sigma}_{LAB}^{\mathrm{traceless}}(\theta,\phi) = -\sigma_{11} \times$$

$$\begin{pmatrix} 1-3\cos^2\phi\sin^2\theta & \frac{3}{2}\sin 2\phi\sin^2\theta & \frac{3}{2}\cos\phi\sin 2\theta \\ \frac{3}{2}\sin 2\phi\sin^2\theta & 1-3\sin^2\phi\sin^2\theta & \frac{-3}{2}\sin\phi\sin 2\theta \\ \frac{3}{2}\cos\phi\sin 2\theta & \frac{-3}{2}\sin\phi\sin 2\theta & 1-3\cos^2\theta \end{pmatrix} \quad (7)$$

In a solid, the θ and ϕ angles are fixed within the range of small lattice vibrations. In an clathrate, guest molecules move inside host cages and have different orientations in the cages at different times. A molecular dynamics simulation of CO_2 guests in a sI clathrate at a temperature *T* gives the orientation of the CO_2 guests in each large cage *i* at different times, *t*. Applying Eq (7), we can determine the chemical shielding tensor, $\boldsymbol{\sigma}_{i,\mathrm{LAB}}(T;t)$, at each time *t* with corresponding eigenvalues $\sigma_{i,xx}(T;t)$, $\sigma_{i,yy}(T;t)$, and $\sigma_{i,zz}(T;t)$. By averaging over all times in a simulation trajectory, averages of the three eigenvalues, $\bar{\sigma}_{i,\alpha\alpha}(T)$ for each cage *i* can be determined.

To simulate the powder spectra for the CO_2 guests, the $\bar{\sigma}_{i,\alpha\alpha}(T)$ for each cage are used to generate a lineshape intensities using the method described by Olivieri[20] Briefly, the frequency for the chemical shift tensor for cage *i*, in the powder spectrum $\sigma_i(\Theta,\Phi)$ is given as,

$$\sigma_i(\Theta,\Phi) = \bar{\sigma}_{i,iso} + (\Delta\bar{\sigma}_i/3)(3\cos^2\Theta - 1 + \bar{\eta}_i\sin^2\Theta\cos 2\Phi) \quad (8)$$

where Θ and Φ are the polar angles which determine the orientations of all cages to the external magnetic field $\mathbf{B}_0$ in a powder sample and $\Delta\sigma = \sigma_{33} - (\sigma_{22} - \sigma_{11})/2$ and $\eta = (\sigma_{22} - \sigma_{11})/\Delta$. The peak intensity for each cage is obtained by binning the values of the chemical shielding, $\sigma_i(\Theta,\Phi)$ in a grid of 1000 points with respect to the values of cosΘ and 360 points corresponding to values of Φ. Further details are described in Ref. [20]. The lineshapes for all cages *i* in the simulation cell are added up as required to generate an overall powder pattern for the sample.

In the simulation setup, the external magnetic field $\mathbf{B}_0$ is chosen to be parallel to the *z*-axis of the cubic simulation cell. At 400 fs intervals in the 1 ns trajectory of the MD simulation, the angles $\theta_i(t)$ and $\phi_i(t)$ are determined for each guest *i* and $\boldsymbol{\sigma}_{i,\mathrm{LAB}}(T;t)$ and the corresponding three eigenvalues $\sigma_{i,\alpha\alpha}(T;t)$ are calculated from the rotation matrix. For each guest, $\bar{\sigma}_{i,xx}(T)$, $\bar{\sigma}_{i,yy}(T)$, and $\bar{\sigma}_{i,zz}(T)$ values are calculated by averaging the $\sigma_{i,\alpha\alpha}(T;t)$ over time. At each temperature, if the average chemical shielding tensor eigenvalues have not converged to within 5 ppm, the simulation is extended a further 1 ns until this convergence criterion is met. The converged, time-

averaged cage eigenvalues are then subjected to the powder averaging of Eq. 8 to generate a powder average spectral lineshape for that cage. All cage lineshapes are added to give the simulated sample lineshape at each temperature.

COMPUTATIONAL METHODOLOGY

The chemical shielding tensor for the isolated CO_2 guest molecules in the PA frame is calculated using the Gaussian 03 suite of programs[21] with the gauge-invariant atomic orbital (GIAO) method[22-25] at the MP2/6-311++G(*d*,*p*) level of theory. To determine the magnitude of the dipolar coupling between the guest and host cage, the chemical shielding tensor for CO_2 guests in isolated sI clathrate small cages at the HF/6-31+G(*d*) level were also performed. Calculations were performed for the guest placed at the center of the cage and displaced by 0.2 Å from the center of the cage with three mutually perpendicular orientations for the CO_2 molecule.

Molecular dynamics simulations are performed with force fields developed in our previous simulations on clathrate hydrates.[26] Water and carbon dioxide molecule are considered rigid with intermolecular potentials taken as the sum of van der Waals (Lennard-Jones 12-6) and electrostatic point charge potentials centered on the carbon and oxygen atoms,

$$V = \sum_{i \neq j} \left\{ 4\varepsilon_{ij} \left[\left(\frac{\sigma_{ij}}{r_{ij}} \right)^{12} - \left(\frac{\sigma_{ij}}{r_{ij}} \right)^{6} \right] + \frac{q_i q_j}{4\pi\varepsilon_0 r_{ij}} \right\}. \quad (9)$$

Point charges q_i and q_j located on the atomic nuclei i and j on different molecules are used to model electrostatic intermolecular interactions. Lennard-Jones potential parameters between unlike atom-type force centers are calculated using, $\varepsilon_{ij} = (\varepsilon_{ii}\ \varepsilon_{jj})^{1/2}$ and $\sigma_{ij} = (\sigma_{ii}+\sigma_{jj})/2$. The extended simple point charge (SPC/E) model is used for water[27] and carbon dioxide Lennard-Jones parameters are taken from the model of Harris and Yung.[28] Point charges on CO_2 were chosen to reproduce the experimental gas phase quadrupole moment of –4.3 esu cm^2.[29,30] The intermolecular potential parameters used in the simulations are given in Table 1.

To equilibrate the initial configurations of the sI CO_2 clathrate, isotropic NPT molecular dynamics simulations with the Nosé-Hoover barostat algorithm[31,32] were performed on a periodic 3×3×3 (35.8 Å per side initial dimensions) replica of the cubic sI clathrate hydrate cage with the DL_POLY 2.17 molecular dynamics program.[33] The simulation cell has a total of 162 large cages and 54 small cages with one CO_2 guest per cage. Three temperatures 77, 150, and 238 K at ambient pressure, and 274 K at 35 bar, were simulated. Thermostat and barostat relaxation times of 0.5 and 2.0 ps, respectively, were used. The equations of motion were integrated with a time step of 1 fs using the Verlet leapfrog algorithm.[34,35] Long-range electrostatic interactions were calculated using the Ewald summation method[34,35] and all intermolecular interactions were calculated within a cutoff distance of R_{cutoff} = 15.0 Å. A total simulation time of 100 ps is used with an initial temperature scaled equilibration period of 30 ps. To obtain the angular distributions of the CO_2 molecules in the large cages at different temperatures, NVE simulations were performed for a minimum total simulation time of 1 ns, starting with configurations equilibrated by the previous NPT runs. If the ensemble averages of the eigenvalues of the chemical shielding tensor for each cage had not converged within this 1 ns time frame, further runs in 1 ns increments were performed until convergent eigenvalues were obtained.

Table 1. Electrostatic point charges and Lennard-Jones interaction parameters for SPC/E water and carbon dioxide.

Atoms	q / e	σ_{ii} / Å	ε_{ii} / kJmol^{-1}
O (water)	-0.8476	3.166	0.6502
H (water)	+0.4238	0.000	0.0000
C	+0.6645	2.785	0.2411
O	-0.33445	3.064	0.6901

RESULTS AND DISCUSSION

The calculated eigenvalues of the NMR chemical shielding and shift tensors for gas-phase CO_2 in the PA frame are given in Table 2. The calculated isotropic chemical shift of CO_2 with respect to TMS is ~125 ppm, which is in excellent agreement with the experimental value of 124 ppm.[36]

To estimate the effect of dipolar coupling of the guest with the cage atoms, the chemical shielding tensor of CO_2 was calculated at the center of a sI small clathrate cage in three mutually perpendicular orientations. The eigenvalues of the chemical shielding tensor σ_{ii} from these three

configurations differed from the free CO_2 molecule by a maximum of 3.3 ppm. The σ_{ii} for three configurations with the CO_2 guest displaced by 0.2 Å from the center of the cage (along the *x*-direction) were also calculated and the values differed from the free CO_2 eigenvalues by a maximum of 3.5 ppm. The σ_{ii} of the guests were not appreciably affected by encapsulation in the clathrate cages and the assumption of only retaining angular dependence in determining the calculated chemical shielding tensor is reasonable.

Table 2. Calculated eigenvalues of the ^{13}C NMR chemical shielding tensors for isolated CO_2 at the MP2/6-311++G(*d*,*p*) and HF/6-31+G(*d*) levels. The chemical shielding of CO_2 inside isolated sI clathrate small cages at the HF/6-31+G(*d*) level for several placements of the CO_2 guest in the sI small cage are also given. The displacement of the guest from the center of the cage (in the *x*-direction), the θ, and ϕ angles are given for each case.

Atoms	σ_{11}	σ_{33}	σ_{iso}
MP2	-39.0	285.6	68.6
HF	-24.0	284.2	78.7
0 Å, 90°, 0°	-23.4, -22.4	280.9	78.3
0 Å, 90°, 90°	-23.2, -22.8	281.6	78.6
0 Å, 0°, 0°	-23.3, -22.6	281.1	78.4
0.2 Å, 90°, 0°	-23.5, -22.5	280.7	78.2
0.2 Å, 90°, 90°	-22.4, -22.1	282.9	79.4
0.2 Å, 0°, 0°	-21.2, -20.7	282.4	80.2

The experimental ^{13}C NMR shifts for solid α-phase carbon dioxide[37] and the CO_2 clathrates[2, 3,7-10] have been reported. At 77 K, the NMR spectrum of solid CO_2 has an observed span Ω = 335 ppm.[12,37] Our calculated value for the span for free CO_2 is 326 ppm which is in good agreement with the experimental result.

Superimposed snapshots at multiple time intervals of the rotational motion of a CO_2 guest molecule in a large cage from MD simulations at three temperatures are shown in Figure 2. At 77 K, the range of the polar angle θ is relatively small and the distribution around ϕ, (the angle in the equatorial plane of the cage) is not homogenous. At low temperatures, the rotation of the CO_2 guests in the large cages about the equatorial plane is hindered which suggests a hopping mechanism for the rotation of the CO_2 guest about ϕ. At the high temperature limit (238 K), the distribution about the ϕ-angle is homogenous (free rotation about the equatorial plane) with a broader range of θ–angles. At 150 K, the distribution about the ϕ-angle is more uniform than the 77 K simulation, but not totally isotropic. Both hopping and hindered rotational motion mechanisms are operating at this temperature.

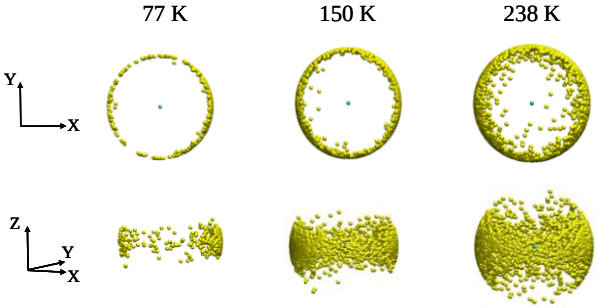

Figure 2. Snapshots of the orientations of a CO_2 molecule in a large sI clathrate cage at 77, 150, and 238 K from MD simulations with the carbon atoms superimposed.

To determine the ^{13}C NMR lineshape for the sI clathrate sample, the *z*-direction of the simulation cell is chosen as the direction of the magnetic field with which the θ-angle is measured. Additionally, the ϕ-angle is referenced with respect to the *x*-axis of the simulation cell. These are the reference directions for calculating the NMR powder lineshape. The cage powder lineshape intensities are superimposed to get the overall sample lineshapes at different temperatures which are shown in Figure 3. No additional line broadening was applied when summing the individual cage spectra to get the sample spectrum.

The calculated high temperature (274 K and 35 bar) spectrum is compared with the experimental results[3] in Figure 3(a). At this temperature, a long simulation time of 5 ns was needed for the convergence of the cage eigenvalues. Excellent agreement between the experimental and calculated results is observed.

The temperature dependence of the lineshapes at 77, 150, and 238 K shown in Figure 3(b) agrees very well with the experimental temperature dependence given in Ref. [12] and shown schematically in Figure 1. The span of the spectra decreases as the temperature increases and the skew is reversed in going from the low to the high temperature limit.

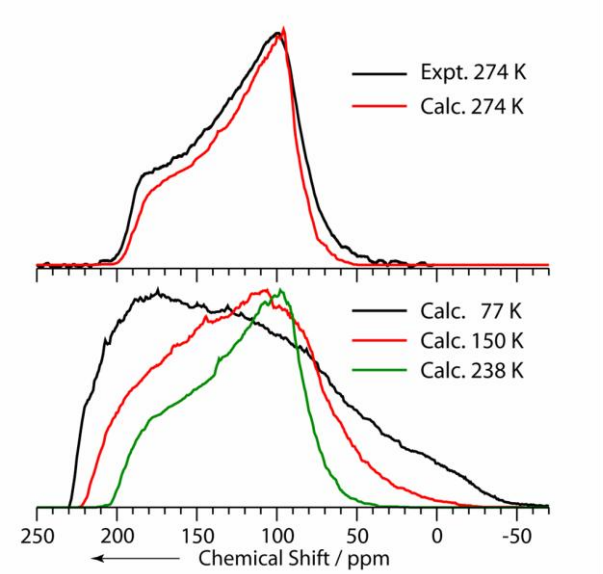

Figure 3. (Top panel) The simulated and experimental ^{13}C powder NMR lineshape at 274 K and 35 bar for CO_2 in the small sI cages. Simulated lineshapes at ambient pressure are given in the bottom panel.

The high temperature CO_2 motion was previously been modeled[14] by the precession of the CO_2 guest with a maximum range of 31° about the equatorial plane. This range is in good agreement with the width spatial distribution of the CO_2 guests obtained in the simulation. In the MD simulations, the range of guest motion was determined without the need to input the experimental lineshape or make any assumption regarding the nature of the motion at this temperature.

As seen in Figure 2, at low temperatures the rotational motion of the guests is hindered and furthermore, the cage water molecules are rotationally frozen. This leads to greater inhomogeniety in the large cage environments and broader NMR powder lineshapes. At high temperatures (238 K), CO_2 guests are rotationally free with respect to rotation in the ϕ-angle and the water hydrogen distributions between the clathrate water oxygens is truly disordered due to rotation of water molecules in the clathrate sites. As a result, the guest peaks are narrower and the skew is reversed compared to the low temperature spectrum. In simulations performed for this study, the longest trajectory time considered is 6 ns. This simulation time is short compared to the time scale of the NMR experiment and the water proton rearrangements. The simulations will therefore not show the total extent of the peak sharpening as the temperature is increased.

SUMMARY AND CONCLUSIONS

A general method for calculating the chemical shift lineshape anisotropy of guest molecules in clathrate hydrate compounds from molecular dynamics simulations has been developed for the case of weak host – guest dipolar coupling. The orientational distributions from molecular dynamics simulation along with time and powder angle averaging are used to calculate the cage chemical shielding tensors and the NMR lineshape produced by each guest molecule. The total predicted lineshape anisotropy is calculated from the superposition of the lineshapes of all guests. The approach is applied to calculate the temperature dependent ^{13}C NMR lineshape anisotropy of carbon dioxide in sI clathrates. The resulting lineshapes agree well with the experimental ^{13}C NMR spectrum at each temperature. The method provides a uniform procedure to calculate the lineshapes at different temperatures and no prior assumptions about the nature of the motion of the guest in cages needs to be made.

REFERENCES

[1] Lee H, Lee JW, Kim DY, Park J, Seo YT, Zeng H, Moudrakovski IL, Ratcliffe CI, Ripmeester JA. *Tuning clathrate hydrates for hydrogen storage.* Nature (London) 2005, 434; 743-746.

[2] Lee H, Seo Y, Seo YT, Moudrakovski IL, Ripmeester JA. *Recovering methane from solid methane hydrate with carbon dioxide.* Angew. Chem. Int. Ed. 2003, 42, 5048-5051.

[3] Park Y, Kim DY, Lee JW, Huh DG, Park KP, Lee J, Lee H. *Sequestering carbon dioxide into complex structures of naturally occuring gas hydrates.* Proc. Natl. Acad. Sci. USA 2006, 103, 12690-12694.

[4] Florusse LJ, Peters CJ, Schoonman J, Hester KC, Koh CA, Dec SF, Marsh KN, Sloan ED. *Stable low-pressure hydrogen clusters stored in binary clathrate hydrate.* Science 2004, 306; 469-471.

[5] Senadheera L, Conradi MS. *Rotation and diffusion of H_2 in hydrogen-ice clathrate by ^1H NMR.* J. Phys. Chem. B 2007, 111, 12097-12102.

[6] Ida T, Mizuno M, Endo K. *Electronic stat of small and large cavities for methane hydrate.* J. Comput. Chem. 2002, 23, 1071-1075.
[7] Ripmeester JA, Ratcliffe CI. *The diverse nature of dodecahedral cages in clathrate hydrates as revealed by ^{129}Xe and ^{13}C NMR spectroscopy: CO_2 as a small-cage guest.* Energy Fuels 1998, 12, 197-200.
[8] Seo YT, Lee H. *Structure and guest distribution of the mixed carbon dioxide and nitrogen hydrates as revealed by X-ray diffraction and ^{13}C NMR spectroscopy.* J. Phys. Chem. B 2004, 108, 530-534.
[9] Kim DY, Lee H. *Spectroscopic identification of the mixed hydrogen and carbon dioxide clathrate hydrate.* J. Am. Chem. Soc. 2005, 127, 9996-9997.
[10] Yeon SH, Seol J, Lee H. *Structure transition and swapping pattern of clathrate hydrate driven by external guest molecules.* J. Am. Chem. Soc. 2006, 128, 12388-12389.
[11] Potrzebowski MJ, Kazmierski S, in New Techniques In Solid-State NMR, Vol. 246, 2005, pp. 91-140.
[12] Ratcliffe CI, Ripmeester JA. *^{1}H and ^{13}C NMR studies on carbon dioxide hydrate.* J. Phys. Chem. 1986, 90, 1259-1263.
[13] Hayashi S. *NMR study of dynamics and evolution of guest molecules in kaolinite/dimethyl sulfoxide intercalation compound.* Clays Clay Miner. 1997, 45, 724-732.
[14] Davidson DW, Ratcliffe CI, Ripmeester JA. *^{2}H and ^{13}C NMR study of guest molecule orientation in clathrate hydrates.* J. Inclus. Phenom. 1984, 2, 239-247.
[15] Harris RK. *Nuclear Magnetic Resonance Spectroscopy*. Essex: Longman, 1989.
[16] Mason J. *Conventions for the reporting of nuclear magnetic shielding (or shift) tensors suggested by participants in the NATO ARW on NMR shielding constants at the University of Maryland, College Park, July 1992.* Solid State Nucl. Magn. Reson. 1993, 2, 285-288.
[17] Seelig J. *Deuterium magnetic resonance: theory and application to lipid membranes.* Q. Rev. Biophys. 1977, 10, 353-418.
[18] Wittebort RJ, Olejniczak ET, Griffin RG. *Analysis of deuterium nuclear magnetic resonance line shapes in anisotropic media*. J. Chem. Phys. 1987, 86, 5411-5420.
[19] Arfken G. *Mathematical Methods for Physicists, 3rd edition*. Orlando: Academic Press, 1985.
[20] Olivieri AC. *How to write a program to simulate solid-state NMR line shapes.* Concepts in Magn. Reson. 1996, 8, 279-292.
[21] Frisch MJ, Trucks GW, Schlegel HB, Scuseria GE, Robb MA, Cheeseman JR, Montgomery Jr. JA, Vreven T, Kudin KN, Burant JC, Millam JM, Iyengar SS, Tomasi J, Barone V, Mennucci B, Cossi M, Scalmani G, Rega N, Petersson GA, Nakatsuji H, Hada M, Ehara M, Toyota K, Fukuda R, Hasegawa J, Ishida M, Nakajima T, Honda Y, Kitao O, Nakai H, Klene M, Li X, Knox JE, Hratchian HP, Cross JB, Bakken V, Adamo C, Jaramillo J, Gomperts R, Stratmann RE, Yazyev O, Austin AJ, Cammi R, Pomelli C, Ochterski JW, Ayala PY, Morokuma K, Voth GA, Salvador PA, Dannenberg JJ, Zakrzewski VG, Dapprich S, Daniels AD, Strain MC, Farkas O, Malick DK, Rabuck AD, Raghavachari K, Foresman JB, Ortiz JV, Cui Q, Baboul AG, Clifford S, Cioslowski J, Stefanov B, Liu G, Liashenko A, Piskorz P, Komaromi I, Martin RL, Fox DJ, Keith T, Al-Laham MA, Peng CY, Nanayakkara A, Challacombe M, Gill PMW, Johnson B, Chen W, Wong MW, Gonzalez C, Pople JA. Gaussian 03, Revision C.02. 2004, Gaussian, Inc.
[22] Ditchfield R. *Self-consistent perturbation theory of diamagnetism I. A gauge-invariant LCAO method for NMR chemical shifts.* Mol. Phys. 1974, 27, 789-807.
[23] Wolinski K, Hinton JF, Pulay P. *Efficient implementation of the gauge-independent atomic orbital method for NMR chemical shift calculations.* J. Am. Chem. Soc. 1990, 112, 8251-8260.
[24] Rauhut G, Puyear S, Wolinski K, Pulay P. *Comparison of NMR shieldings calculated from Hartree-Fock and density functional wave functions using gauge-including atomic orbitals.* J. Phys. Chem. 1996, 100, 6310-6316.
[25] Cheeseman JR, Trucks GW, Keith TA, Frisch MJ. *A comparison of models for calculating nuclear magnetic resonance shielding tensors.* J. Chem. Phys. 1996, 104, 5497-5509.
[26] a) Alavi S, Ripmeester JA, Klug DD. *Molecular dynamics study of structure II hydrogen clathrates*. J. Chem. Phys. 2005, 123; 024507-1-024507-7; b) Alavi S, Ripmeester JA, Klug DD. *Molecular dynamics simulations of binary structure II hydrogen and tetrahydrofuran clathrates*. J. Chem. Phys. 2006, 124; 014704-1-014704-6; c) Alavi S, Ripmeester JA, Klug DD. *Molecular dynamics simulations of binary*

structure H hydrogen and methyl-tert-butylether clathrate hydrates. J. Chem. Phys. 2006, 124; 204707-1-204707-8; d) Alavi S, Ripmeester JA, Klug DD. *Molecular dynamics study of the stability of methane structure H clathrate hydrates.* J. Chem. Phys. 2007, 126, 124708; e) Dornan P, Alavi S, Woo TK. *Free energies of carbon dioxide sequestration and methane recovery in clathrate hydrates.* J. Chem. Phys. 2007, 127, 124510; f) Alavi S, Woo TK. *How much carbon dioxide can be stored in the structure H clathrate hydrates? : A molecular dynamics study.* J. Chem. Phys. 2007, 126, 044703.

[27] Berendsen HJC, Grigera JR, Straatsma TP. *The missing term in effective pair potentials.* J. Phys. Chem. 1987, 91, 6269-6271.

[28] Harris JG, Yung KH. *Carbon dioxide's liquid-vapor coexistence curve and critical properties as predicted by a simple molecular model.* J. Phys. Chem. 1995, 99, 12021-12024.

[29] Etters RD, Kuchta B. *Static and dynamic properties of solid CO_2 at various temperatures and pressures.* J. Chem. Phys. 1989, 90, 4537-4541.

[30] Buckingham AD, Disch RL. *The quadrupole moment of the carbon dioxide molecule.* Proc. Roy. Soc. London Ser. A. 1963, 273, 275-289.

[31] Nosé S. *A unified formulation of the constant temperature molecular dynamics method.* J. Chem. Phys. 1984, 81, 511-519.

[32] Melchionna S, Ciccotti G, Holian BL. *Hoover NPT dynamics for systems varying in shape and size.* Mol. Phys. 1993, 78, 533-544.

[33] Forester TR, Smith W. DL_POLY 2.17. 1995, CCLRC

[34] Frenkel D, Smit B, *Understanding Molecular Simulation*. San Diego: Academic Press, 2000.

[35] Allen MP, Tildesley DJ. *Computer Simulation of Liquids*. Oxford: Oxford Science Publications, 1987.

[36] Pouchert CJ. *Aldrich Library of NMR Spectra, 2nd edition*. Milwaukee: Aldrich Chemical Corporation, 1983.

[37] Beeler AJ, Orendt AM, Grant DM, Cutts PW, Michl J, Zilm KW, Downing JW, Facelli JC, Schindler MS, Kutzelnigg W. *Low-temperature carbon-13 magnetic resonance in solids. 3. Linear and pseudolinear molecules.* J. Am. Chem. Soc. 1984, 106, 7672-7676.